Potential Application of Gelatin Scaffolds Prepared through *In-situ* Gas Foaming in Skin Tissue Engineering

S. Ali Poursamar [a]

Javad Hatami [c]

Alexander N. Lehner [b]

Cláudia L. da Silva [c]

Frederico Castelo Ferreira [c]

A.P.M. Antunes [a]

---

[a]: Institute for Creative Leather Technologies, Park Campus, The University of Northampton, Boughton Green Road, Northampton, NN2 7AL, UK.

[b]: Centre for Physical Activity and Chronic Disease and the Aging Research Centre, Institute for Health and Wellbeing, School of Health, Park Campus, The University of Northampton, Boughton Green Road, Northampton, NN2 7AL, UK.

[c]: Department of Bioengineering and IBB, Institute for Bioengineering and Biosciences, Instituto Superior Técnico, Universidade de Lisboa, Av. Rovisco Pais, 1049-001 Lisboa, Portugal.

Correspondence author:

Dr. S.Ali Poursamar
Ali@northampton.ac.uk
Telephone Number: +49 (0)1521036 1278
Fax Number: +44 (0)1604 711183

Abstract: Gelatin's excellent foaming ability allows the application of *in-situ* gas foaming as a preparation technique for porous scaffold development. Here, a new iterative experimental design for *in-situ* gas foaming method is reported. The prepared scaffolds were studied for applying the findings to the future skin tissue engineering scaffolds. The thermal stability, mechanical properties, and pore structure of the scaffolds are reported and their degradation resistance by using collagenase enzyme and their cytotoxicity by using fibroblasts were studied. The results of this study demonstrated that gas foaming method can be modified to produce an interconnected porous structure with enhanced mechanical properties.

Keywords: Gelatin; Wound dressing; Gas foaming; Tensile strength; Cytotoxicity;

1. Introduction

Porosity plays an important role in ensuring the optimum functioning of tissue engineering scaffolds by accelerating metabolite transport and facilitating cell migration and proliferation [1]. This has prompted researchers to constantly envisage more effective methods for obtaining porous scaffolds with better characteristics. Gas foaming is a technique used to prepare scaffolds with a desirable porosity [2]. The term *Gas foaming* may refer to the method of infusing a confined polymeric precursor in liquid state with pressurised gas [3]. However, this method requires expensive hardware and significant investment costs. In order to turn it into a more affordable and accessible technique, gas foaming may be performed in conjunction with an *in-situ* chemical reaction that transforms the liquid precursor into foam and eventually a solid porous structure [4]. The method comprises of a liquid phase, gasified through a thermal decomposition or chemical reaction [5]. Different materials show different abilities to form a stable foam. Materials with suitable surfactant properties usually have a desirable *foaming ability*. Gelatin is well known to possess such ability and hence is a

suitable candidate for being processed via a gas foaming technique [6]. We previously reported the development of a novel variation of *in-situ* gas foaming [7]; however, we observed that a high rate of CO_2 release led to an undesirable low tensile strength of the samples. Therefore the focus of current report explores further optimisation of the process central parameters, with a specific attention to the sequence of gas release.

In the last two decades skin tissue engineering scaffolds have been widely used in commercially-available wound dressings to improve the rate of healing in chronic wounds [8]. Since collagen is the main protein constituent of skin, a significant portion of the commercially available wound management products use collagen to foster skin regeneration [9]. Gelatin results from collagen denaturation and since it retains some of its precursor chemotactic signals (such as RGD amino acid sequence, which promotes cell adhesion [10]), it has been considered as a cost-effective alternative to collagen for the potential application in skin tissue engineering [11, 12]. In this study, the resistance of the prepared scaffolds to collagenase was studied to simulate the digestive environments promoted by this enzyme that exists in chronic wounds. During wound healing, fibroblasts represent one of the major cell types that should successfully proliferate, integrate, and regenerate in the wound area [13]. The response of fibroblasts to the prepared samples was studied *in-vitro* using cytotoxicity assays according to the ISO 10993-5 guidelines. The gelatin molecular structure was studied using Fourier Transform Infra-Red Spectroscopy (FT-IR) and the mechanical properties of the samples were characterised using tensile strength analysis.

2. Materials and Methods

2.1. Scaffold Preparation Method

A previous report on executing *in-situ* gas foaming method showed that initiating the chemical reaction and releasing the gas within the confinement of the mould cause undesirable effects on the pore size distribution of the scaffolds [7]. Under such experimental

conditions, the released gas cannot be vented off from the mould and this will lead to over-pressurisation within the solution which subsequently causes macro bubbles to be formed. Larger bubbles would consequently form a larger pore size in the final structure of scaffolds. In this study, in order to avoid such conditions, the chemical reaction and the subsequent gas release were executed outside the mould and the resulting foam was then injected into the mould to form a final structure. Type B gelatin powder (Sigma Aldrich, USA) was used to prepare 20% w/v gelatin solution in de-ionised water. To initiate foaming, 0.32 g of sodium bicarbonate (BDH Chemical, UK) was added directly to the gelatin solution. After 10 seconds, 360 μl of acetic acid (Fisher Scientific, UK) was added to the solution to react with effervescent phase. The produced gelatin foam was cast in polystyrene moulds (5.5 cm diameter). The moulds were pre-cooled and frozen at -25˚C for 1 hour. The frozen foam blocks were then extracted from the moulds and placed in de-ionised water to extract unreacted components. To crosslink the scaffolds, the samples were then immersed in aqueous solutions of glutaraldehyde (GTA) at concentrations of 0.25, 0.50, 0.75, and 1.00% v/v GTA for 3 hours (adjusted to a pH of 5). The GTA solutions were prepared from a 50% v/v aqueous stock solution of GTA (Fisher Scientific, UK). The samples were washed in de-ionised water overnight, frozen, and lyophilised at -40˚C under a vacuum pressure of 0.250 mbar for a day. Non-crosslinked samples were prepared as a control in absence of the crosslinking step.

2.2. Characterisation of the Prepared Scaffolds

2.2.1. Mechanical Properties

Tensile strength, Young's modulus, and tensile strain of the scaffolds were determined using a Texture Analyzer (TA.XT-Plus, Stable Micro Systems, UK). After conditioning the samples at 20˚C and 95% relative humidity for 2 days, the samples were cut into rectangular strips (10 × 5mm), the thickness was measured at 3 points and the average values were

recorded. The samples were drawn with a cross head speed of 0.033 $mm.sec^{-1}$. The linear segment of Stress-Strain curve was used to determine the Young's modulus and the values reported in kPa. The tensile strength and strain values are reported in kPa and percentage (%), respectively. The tests were performed in triplicate.

2.2.2. Thermal Analysis

Differential Scanning Calorimetry (DSC - 822e, Mettler-Toledo, Switzerland) was used to perform thermal analysis. The samples were conditioned at 65% relative humidity and 20˚C for 2 days, they were cut and sealed in 40 µl aluminum pans. The samples were heated from 15 to 100˚C at a heating rate of $5˚C.min^{-1}$ under inert atmosphere of nitrogen gas. The peak temperature and the normalised enthalpy of transition for each sample were recorded. The peak temperature of thermograph was assigned as the gelatin denaturation temperature (T_d). The normalised enthalpy of transition was computed as the integrated area under the transition peak. The experiments were performed in triplicate.

2.2.3. Fourier Transform Infra-Red Spectroscopy (FT-IR)

Fourier Transform Infra-Red spectroscopy (FTIR/ATR-4800s, Shimadzu, Japan) was performed by scanning from 4000 to 1000 cm^{-1}. The samples were conditioned in a 0% relative humidity desiccator for 2 days prior to analysis. Multiple scans were performed on each sample and a representative FT-IR diagram for each sample is chosen for discussion.

2.2.4. Crosslinking Index

The degree of crosslinking was assessed according to the Ninhydrin Assay method reported by Sun *et al.,* with minor modifications [14]. Briefly, gelatin scaffolds were weighed and added to 2 ml aliquot of 50% v/v aqueous ninhydrin reagent solution. The samples were heated in 100˚C water for 20 minutes. The samples were then cooled at room temperature and 5 ml of 50% v/v ethanol-water solution was added. The samples were vortexed for 15 seconds and the absorption was measured at 570 nm (UV-250IPC, Shimadzu, Japan).

Aqueous solutions of glycine with known standard concentrations were used to plot the calibration curve. The non-crosslinked samples were used to estimate the number of free amine groups available per mass unit of pure gelatin ($N_{non\text{-}crosslinked}$). The crosslinking index is reported as a percentage and defined as the number of free amine groups available in the crosslinked sample ($N_{crosslinked}$) normalised to $N_{non\text{-}crosslinked}$ (Equation 1).

$$\text{Crosslinking Index (\%)} = \frac{N_{crosslinked}}{N_{non-crosslinked}} \times 100 \qquad \text{(Equation 1)}$$

2.2.5. Microstructure Analysis

The scaffolds were examined using a Scanning Electron Microscope (SEM, S-3000N, Hitachi, Japan) operated at 5kV. Samples were gold-coated using a sputter coater (SC500, Mscope, UK). The average pore size of the samples was determined using Quartz PCI image processing software package (Quartz Image Corp., Vancouver, Canada).

2.2.6. *In-Vitro* Biodegradation Assay

Assessing the resistance of a wound dressing against enzymatic degradation may be a useful tool in estimating the biodegradability of scaffold *in-vivo*. Biodegradation assays were carried out using collagenase according to the method described by Melling *et al.* with some modifications [15]. The scaffolds were cut and their dry weights were recorded. Collagenase, from *Clostridium Histolyticum* (125 CDU/mg, Sigma, USA) was dissolved in PBS to obtain concentrations of 2.5 and 5 mg/ml with enzymatic activities of 625 and 317.5 CDU/ml, respectively. The enzyme solution (300 µl) was added to 100 mMol $CaCl_2$ solution (500 µl). The final mixture was diluted to 5 ml total volume with PBS. A set of control samples was prepared by incubating the samples in de-ionised water for comparison. All samples were incubated in an orbital water bath at 40 rpm and 37˚C for a day. The solutions were centrifuged for 5 minutes at 1000g at 5˚C (Megafuge 16R, Thermo Scientific, Germany). The non-digested samples were collected using filter paper No. 541 and dried at 100˚C. The

samples were dried until constant weight (to 2 decimal places). The final constant weight was recorded as the residual non-degraded mass. The degradation ratio was computed for each sample as the ratio of residual non-degraded mass to the initial mass (Equation 2):

$$Degradation\ Ratio\ (\%) = \frac{Residual\ Non-degraded\ Mass}{Initial\ Mass} \times 100 \quad \text{(Equation 2)}$$

2.2.7. Cytotoxicity Analysis

Prior to cytotoxicity analysis, the scaffold samples were sterilised under UV light for 6 hours. The ISO 10993-5 guidelines were used to perform indirect cytotoxicity tests [16]. Briefly, triplicate scaffold samples (3×3×5 mm) were incubated in 2ml Dulbecco's Modified Eagle's Medium (DMEM, Gibco, UK) with 10% v/v of Fetal Bovine Serum (FBS, Gibco, UK) in polystyrene tubes (BD Bioscience, USA) at 37˚C, 5% CO_2, and fully humidified air for 3 days. The liquid extracts were used to culture L929 mouse fibroblast cell line (DSMZ, Germany) with an initial density of 80×10^3 cell/cm^2 in 24-well plates for 3 days. The cell metabolic activity was determined using a MTT (3-[4,5-dimethylthiazol-2-yl]-2,5-diphenyl tetrazolium bromide) cell proliferation kit (Sigma Aldrich, USA). The results were normalised to the negative control (fresh DMEM with 10% FBS medium) and compared with the positive control (medium pre-incubated with latex).

2.2.8. Statistical Analysis

Non-parametric tests were undertaken using the Kruskal-Wallis Method with SPSS Statistics software (Ver. 20, IBM, NY, USA). The analysis showed the presence of any significant differences amongst the results at $p \leq 0.05$.

3. Results

3.1. Mechanical Properties

Table 1 lists the tensile properties of the scaffolds crosslinked at different concentrations of GTA. In comparison with the non-crosslinked samples, only the 0.50% v/v GTA concentration significantly increased the scaffolds tensile strength ($p\leq0.05$). The

increase of tensile strength for the samples crosslinked at 0.25% v/v GTA was not significant in comparison with the non-crosslinked samples ($p \leq 0.05$). Similar comparison shows that crosslinking at concentrations higher than 0.50% v/v significantly decreased the tensile strength of scaffolds ($p \leq 0.05$).

Table 1: Tensile properties of the prepared gelatin scaffolds at various GTA concentrations. The tensile strain of the scaffolds was reduced as a result of crosslinking. Results are shown as an average ± standard deviation.

GTA Concentration (% v/v)	Tensile Strength (kPa)	Young's Modulus (kPa)	Tensile Strain (%)
0.00	80.76 (±4)	0.87 (±0.1)	114.83 (±9)
0.25	100.10 (±13)	2.09 (±0.1)	38.57 (±1)
0.50	239.48 (±70)	2.44 (±0.4)	30.23 (±5)
0.75	59.22 (±14)	1.80 (±0.1)	30.02 (±0.4)
1.00	15.46 (±5)	4.07 (±1.3)	17.88 (±5)

As the result of crosslinking, the Young's modulus of the scaffolds was increased from 0.87 kPa in the non-crosslinked samples to higher values in all of the crosslinked scaffolds. The scaffolds crosslinked with 1% v/v GTA had the highest Young's modulus (4.07 kPa), which was significantly higher than the non-crosslinked samples ($p \leq 0.05$).

The tensile strain of the scaffolds decreased significantly as a result of crosslinking. The non-crosslinked samples showed an elongation value of 114.8%, whilst the scaffolds crosslinked with 1.00% v/v GTA showed the lowest elongation at 17.9% which was significantly less than non-crosslinked samples ($p \leq 0.05$).

3.2. Thermal Analysis

Table 2 lists the thermal characteristics of gelatin scaffolds crosslinked at different concentrations of GTA. As a result of crosslinking the denaturation temperature (T_d) was increased from 48˚C in the non-crosslinked samples to the temperature above 80˚C in all of the crosslinked scaffolds. Denaturation temperature is an indirect measurement of the crosslinking degree. A higher denaturation temperature value delineates a greater degree of crosslinking [17]. As the result of crosslinking, the enthalpy of transition (ΔH) shifted to smaller negative values. The enthalpy of transition was changed from -25.7 $J.g^{-1}$ in the non-crosslinked samples to -12.3 $J.g^{-1}$ in the scaffolds crosslinked with 1% v/v GTA.

Table 2: Thermal analysis of porous gelatin scaffolds crosslinked at different concentrations of GTA. Peak temperature is assigned as T_d in this study. Results are shown as an average ± standard deviation.

GTA concentration (% v/v)	**Denaturation Temperature (T_d) (˚C)**	**Enthalpy of Transition (ΔH) ($J.g^{-1}$)**
0.00	48.1 (± 6.9)	-25.7 (±16.7)
0.25	82.0 (±3.5)	-16.4 (±0.4)
0.50	84.5 (± 1.5)	-16.3 (±0.9)
0.75	86.2 (±1.6)	-13.2 (±3.2)
1.00	83.8 (±1.4)	-12.3 (±1.8)

3.3. Fourier Transform Infra-Red Spectroscopy (FT-IR)

Figure 1 compares the FT-IR spectra of gelatin scaffolds crosslinked at different GTA concentrations. Gelatin amide absorptions are noticeable in all of the non-crosslinked and crosslinked spectra. This includes amide I, II, and III at 1633, 1540, and 1238 cm^{-1}, respectively. The amide A and B absorptions were evident at 3400 and 3050 cm^{-1}, respectively. Carbon and oxygen atoms interactions as part of the gelatin carbonyl groups (C=O) cause the Amide I absorption [18]. N-H bending and N=C stretching in amide linkages are responsible for both the amide II and amide III absorptions [19]. Amide A and

amide B are assigned to the vibrations of hydroxyl groups (O-H) and N-H stretching vibrations, respectively [20]. An absorption peak at 3425 cm^{-1}, which corresponds to the -OH stretching band [21], is noticeable in the non-crosslinked samples spectrum but it was absent from the spectra of crosslinked scaffolds.

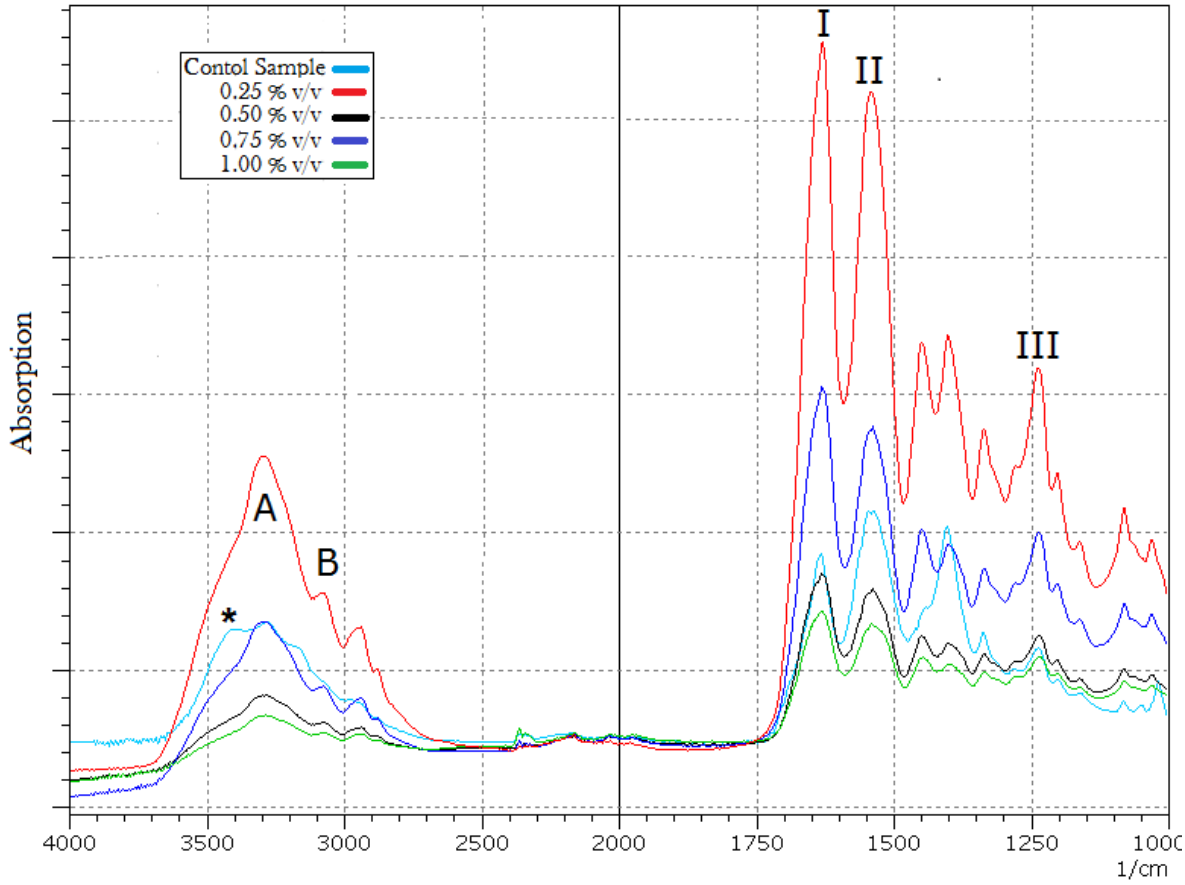

Fig. 1 The FT-IR spectra of non-crosslinked and crosslinked samples. The shoulder-like absorption at 3425 cm^{-1} (marked by *) was visible in the non-crosslinked samples and was absent in the crosslinked samples. This absorption band represents -OH hydroxyl functional groups and its disappearance may be indicative of OH functional groups consumption during the crosslinking process

3.4. Crosslinking Index

Figure 2 compares the change in the degree of crosslinking index as a function of GTA concentration. GTA solution with a concentration of 0.25% v/v crosslinked 92% of the free amine groups when compared with non-crosslinked samples. Increasing GTA concentration

above this value did not change the crosslinking index significantly ($p \geq 0.05$). Therefore crosslinking of gelatin scaffolds with GTA appeared to have been optimised at 0.25% v/v GTA.

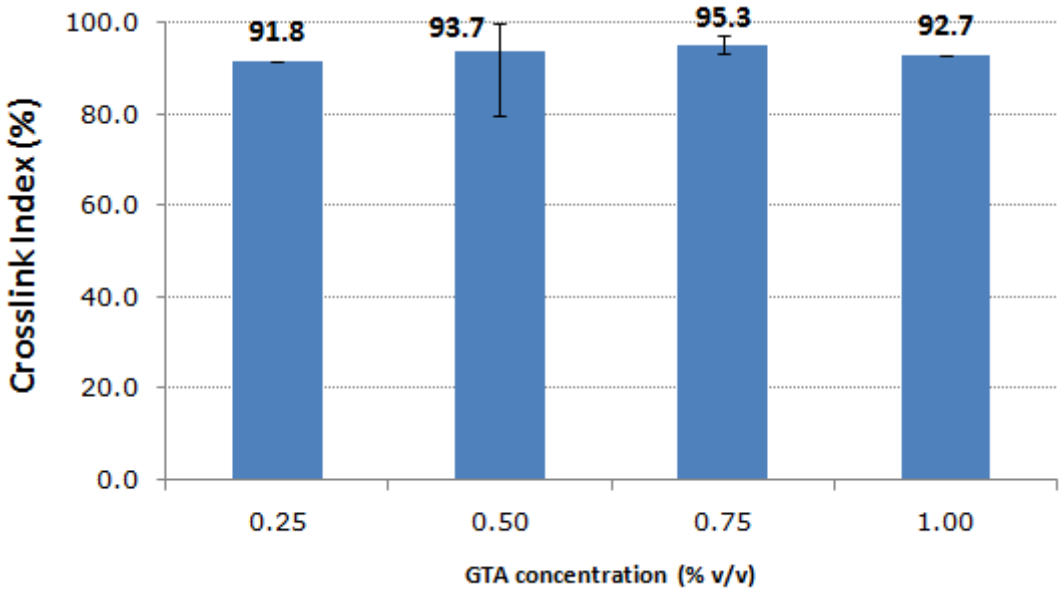

Fig. 2 The crosslink index is reported as the number of free amine groups available in the crosslinked sample normalised to the number of free amine groups in non-crosslinked scaffolds. The crosslink index stayed stable above 90% value, regardless of GTA concentration

3.5. Microstructure Analysis

Figure 3 (A-F) displays the microstructure of the porous gelatin scaffolds. The structure of the prepared scaffolds showed an inter-connected porous matrix. The average pore size for the non-crosslinked scaffolds was 180µm. The scaffolds crosslinked with 0.50 and 1% v/v GTA showed an average pore size of 233µm and 306µm, respectively. Due to softness and plastic properties of the non-crosslinked scaffolds (as reported in Section 3.1), sectioning and preparation of samples for SEM analysis caused distortion of pores for this set of samples (Figure 3-A). The microstructure of the crosslinked scaffolds showed

interconnectivity which is critical for cell migration and proliferation and facilitating the exchange of nutrients and waste products [22].

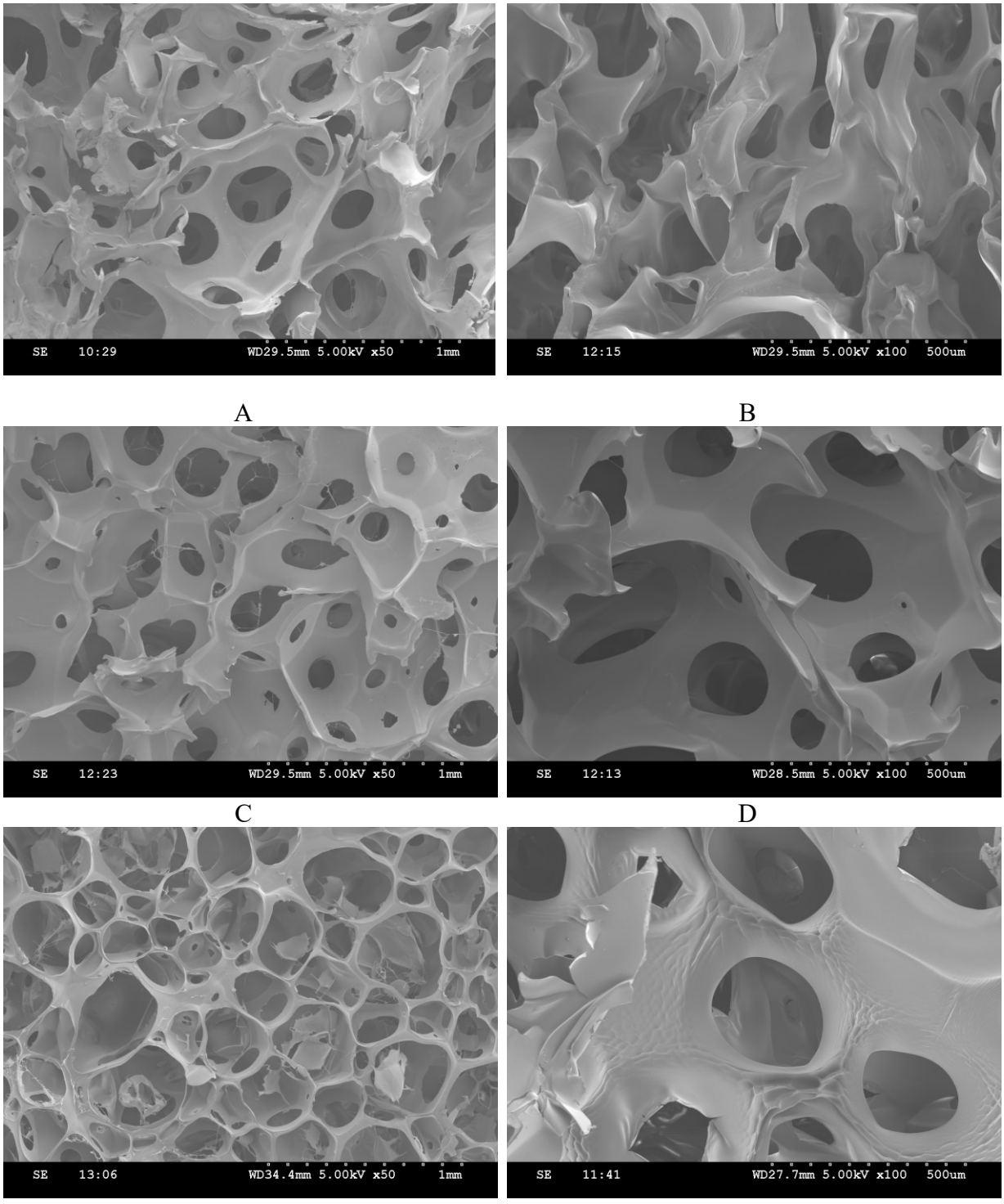

Fig. 3 SEM images at 50x and 100x magnifications showing interconnectivity and the pore structure of gelatin scaffolds as a function of GTA concentration (0% to 1% v/v). (A, B) non-crosslinked samples; (C, D) scaffolds crosslinked with 0.50% v/v GTA solution; (E, F), scaffolds crosslinked with 1% v/v GTA solution

3.6. *In-Vitro* Biodegradation Assay

Figure 4 shows the results of the biodegradation analysis performed using two different collagenase concentrations (119 and 234 CDU/ml) in comparison with a set of control samples that were incubated in de-ionised water only. In the absence of enzyme, crosslinking samples at all concentrations of GTA sufficiently stabilised the gelatin scaffolds in 37˚C de-ionised water for a day. However, upon the addition of enzyme, a noticeable difference between the effects of different GTA concentrations on the scaffolds stability was observed. At a collagenase concentration of 119 CDU/ml, the degradation rate of the samples crosslinked with 0.25% v/v GTA was 39.5% of the initial mass after a day of enzymatic hydrolysis. At GTA concentrations greater than 0.25% v/v, less than 10% of the samples initial mass was degraded during the same incubation period. At higher concentration of collagenase (234 CDU/ml), after a day of incubation with the enzyme, 91% of initial mass of scaffolds crosslinked at 0.25% v/v GTA was degraded and the scaffolds crosslinked with 1% v/v GTA showed a degradation rate of less than 30% of the initial mass.

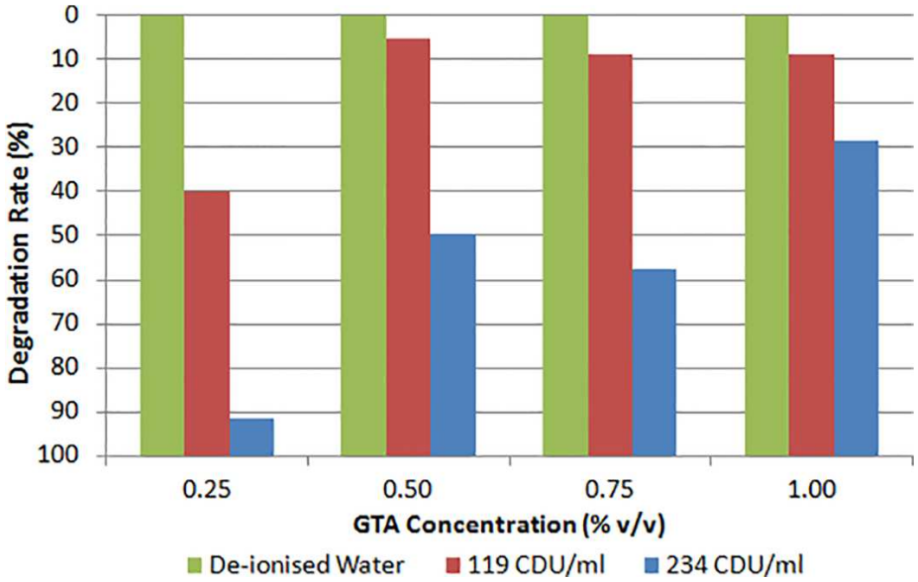

Fig. 4 The results of *in-vitro* biodegradation analysis using collagenase enzyme as a function of GTA concentrations. These results are compared with a set of control samples that were incubated in 37˚C de-ionised water without enzyme

3.7. Cytotoxicity Evaluation

L929 cells metabolic activities were assessed in an indirect cytotoxicity test according to the ISO 10993-5 guidelines. Cytotoxicity results were normalised to the negative control and compared with the positive control (Figure 5). At the lowest GTA concentration, there was a 10% increase in toxicity level, whilst at the greatest GTA concentration, there was a 32% increase in the cytotoxicity level. However, the reduction of cell viability as a result of crosslinking was not statistically significant ($p \geq 0.05$).

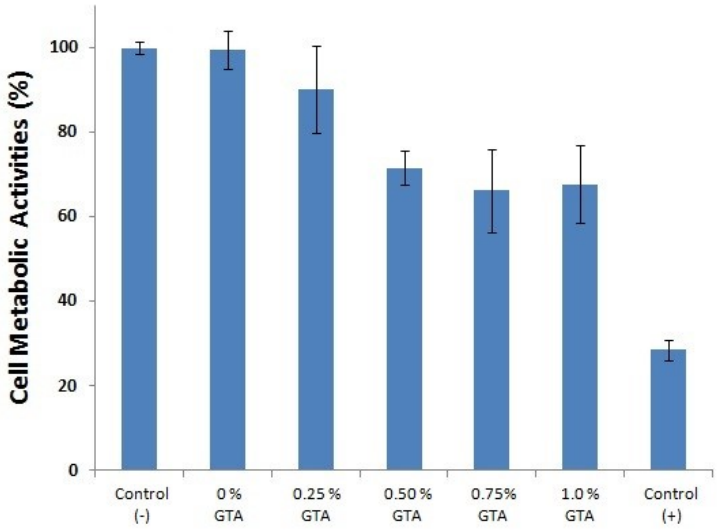

Fig. 5 Cell metabolic activity as measured in an indirect cytotoxicity test. Results are normalised to the negative control and compared with the positive control. Results are shown as an average ± standard deviation

4. Discussion

Due to both the aging population (longer lifespan) and the concurrent increase in comorbidities such as diabetes, obesity, and peripheral vascular diseases, the incidence of chronic wounds has been growing in developed countries. Treatment of such wounds imposes an increasing burden on the healthcare budget of these countries. In the UK alone, the allocated annual budget for the chronic wound management is estimated to top £3 billion [23]. Manufacturing smarter and more effective wound dressings may be instrumental in

improving life quality of the affected population and bringing the costs of wound management under control. In the past two decades, a new generation of wound dressings have been developed that employs the principles of tissue engineering for treatment and management of chronic wounds [8]. Advanced wound dressings are capable of supporting cell growth and they may safely be implanted and left *in-situ* in the skin after successful tissue regeneration [24]. To support cell growth and successful integration in natural skin tissue, the wound dressings need to provide mechanical support, be porous, and provide chemotactic signals to the surrounding cells [22]. Considering the similarity of gelatin to skin collagen, the former can provide biological recognition signals to cells and by designing structures with desirable mechanical properties, porosity, and *in-vivo* stability, a promising gelatin-based wound dressing for the application in chronic wound treatments may be obtained.

The mechanical strength of human skin differs in various parts of body, and has been reported to be between 0.13 to 0.32MPa in the area of forearms and forehead [25]. In this research study, depending on the applied GTA concentration, the prepared scaffolds showed a maximum tensile strength of 0.24 MPa (Table 1). Although the initial increase of GTA concentrations led to an increase in the tensile strength, there is a limit in the ability of using GTA crosslinking in increasing the tensile strength. Comparing with non-crosslinked samples, the tensile strength of the scaffold reached a maximum at the GTA concentration of 0.50% v/v. Upon further increase of GTA concentration, the strength of scaffold was significantly decreased. Such a decrease in tensile strength at high concentrations of crosslinker has been observed by other researchers [26-28]. It is suggested that such a decline is a result of increasing brittleness and existing porosity which act as points of crack propagation [29]. Price (1986) points to the increase of structural brittleness as the root cause for the decrease in the tensile strength. The observed significantly greater Young's modulus

at high concentrations of GTA was similar to reported results by Price (1986). In porous structures (such as samples in this study), an increase in the brittleness would lead to faster rate of crack growth and structural failure at lower tensile strengths. In comparison with our previous report describing a structures prepared with *in-situ* gas foaming [7], the tensile strength results in Table 1 are noticeably greater, whilst similar comparison with previously reported results shows that the average pore sizes reported in Section 3.5 are lower [7]. Considering the impact of porosity on the tensile strength [29], the relatively higher tensile strength observed in this study may be due to smaller pore structure. This may point to the impact of releasing gas before mould casting on reducing the pore size average and helping in tensile strength increase.

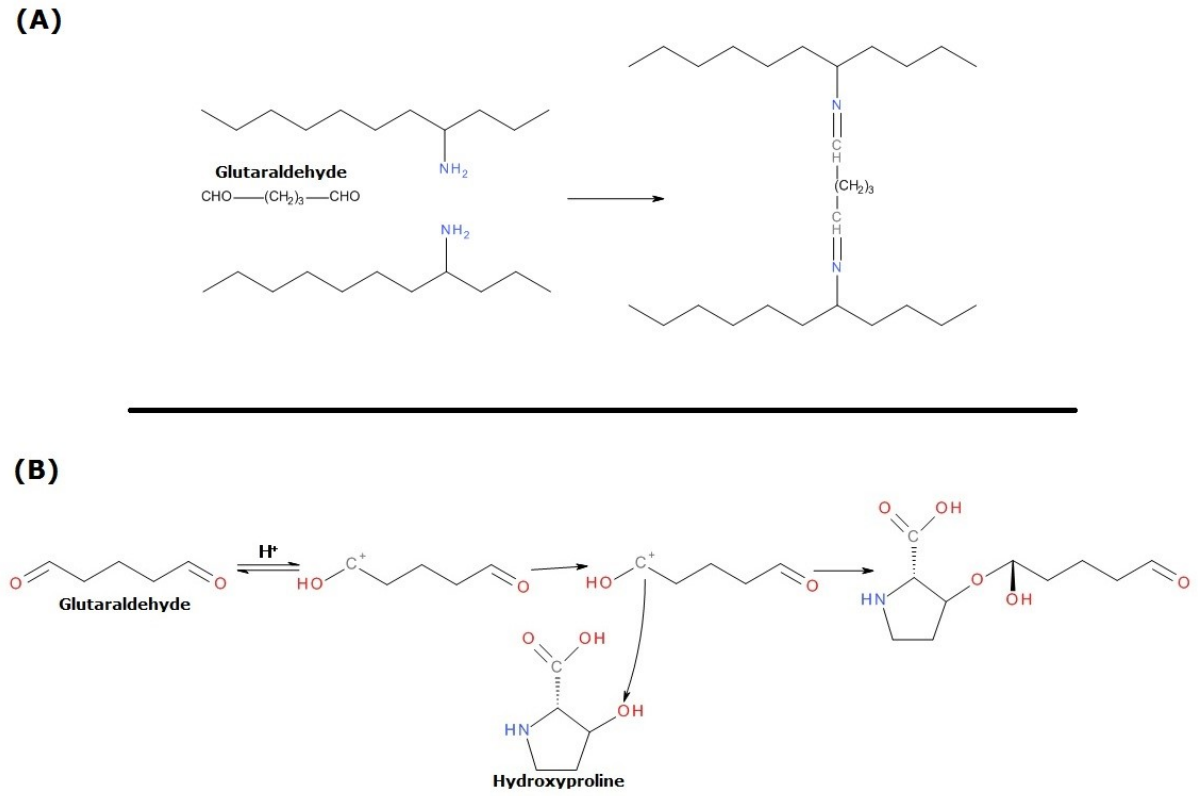

Fig. 6 Proposed reaction mechanism of aldehydic groups with: (A) gelatin amine groups and the formation of C=N bonds [30], (B) proposed GTA reaction with the hydroxyl groups of hydroxyproline at acidic pH's [21].

An increase in mechanical strength of crosslinked structures is a direct result of covalent bonds formation between polymeric macromolecules [21]. The effectiveness of crosslinking and the extent of covalent bond formation after crosslinking can be measured indirectly through thermal analysis. The formation of covalent bonds between the gelatin molecules as a result of crosslinking is responsible for the increase in the denaturation temperature (Table 2) [17]. Denaturation temperature (T_d) is associated with the proteins unfolding and aggregation as a result of heating. The intermolecular restriction in the mobility of gelatin molecules as a result of crosslinking causes the entropy of transition to decrease [31] and thus the denaturation and unfolding of the protein molecules require higher amount of energy and therefore a higher temperature to proceed [32]. An increase of denaturation temperature confirms crosslinking within the gelatin structure. The FT-IR results may provide further additional information with regards to the mechanism of gelatin crosslinking with GTA (Figure 1). The main reaction of GTA with gelatin includes establishment of covalent bonds between the amine groups of lysine (hydroxylysine). It is suggested that the prominent GTA reaction mechanism is the Schiff base reaction [33] and includes the establishment of carbon and nitrogen double bonds (C=N) between GTA and gelatin molecules (Figure 6-A). At acidic pH's, this reaction is less probable due to the protonation of amine groups [21]. Farris *et al.* (2010) suggested an alternative reaction mechanism for GTA reaction with proteins under acidic pH's. According to Farris *et al.* (2010) at low pH's the crosslinking may be carried out through the protonation of the carbon in the GTA aldehydic group with the subsequent reaction with -OH groups of hydroxyproline and hydroxylysine, resulting in the formation of ether bonds [21]. Figure 6-B illustrates the proposed aldehyde reaction with hydroxyproline at acidic pH's. In Figure 1, in the absence of a crosslinker, there is a shoulder-like absorption band at 3425 cm^{-1} which corresponds to the gelatin -OH stretching band. However, for the crosslinked samples, this absorption band

almost disappeared which suggests the -OH group may have been involved in the reaction with the GTA. Figure 1 may show that GTA reaction with hydroxyl functional groups was involve in crosslinking mechanism.

In order to assist the closure of wounds, an optimal wound dressing should be resistant to the surrounding digestive conditions that prevail in the early stages of wound healing. The wound healing stages may be divided into four phases that occur in the following chronological order: Haemostasis, Inflammation, Proliferation, and Remodeling [34]. The inflammation phase is marked by a high activity of matrix metalloprotase enzymes (MMP's) such as collagenase, whilst the next phase (proliferation) is marked by rapid fibroblast growth and migration into the injured area. An effective wound dressing needs to withstand the inflammation phase of wound healing with resistance to degradation until the beginning of the proliferation phase which is expected three days after initial injury [34]. For this to occur, a rate of less than 30% mass degradation per day is desirable. The rate of scaffold degradation was a function of enzyme concentration, as it is shown in Figure 4. Whilst the majority of the crosslinked scaffolds showed degradation rate of less than 30% mass degradation per day at the collagenase concentration of 119 CDU/ml, at the highest concentration of collagenase (234 CDU/ml), only the scaffolds crosslinked with 1% v/v GTA exhibited a degradation rate of less than 30% mass degradation per day. There are qualitative and quantitative differences amongst the digestive components of different types of chronic wounds; for instance, chronic venous ulcers show higher content and diversity of MMP enzymes than pressure ulcers [35]. Whereas the scaffolds crosslinked with low range of GTA concentrations can be resistant against moderate digestive wound environments, the application of 1% v/v GTA crosslinking is necessary for a highly digestive wound environment such as venous ulcers. Despite higher resistance against degradation, cytotoxicity evaluations showed that scaffolds crosslinked with 1% v/v GTA were three times

more toxic than the samples crosslinked with 0.25% v/v GTA. This reaffirms the need to find a less cytotoxic crosslinker than GTA in order to have both acceptable *in-vivo* stability and a satisfying biocompatibility. It should be pointed out that this research study was mainly aimed at optimising the *in-situ* gas foaming method and GTA was used as a model crosslinker for this purpose. Further studies on applications of alternative crosslinkers will be the subject of future studies.

5. Conclusion

In this study, a porous gelatin scaffold with an inter-connected porous system was prepared using *in-situ* gas foaming optimisation. The recommended pore size range for skin tissue engineering scaffolds is reported to be 20-125μm [2]. In this study, the prepared scaffolds showed an average pore size more similar to this optimum range than previous report on the outcome of *in-situ* gas foaming application [7]. The prepared scaffolds showed a relatively similar tensile strength to human skin that protects the areas of forehead and forearm. A limit was detected in the ability of GTA in increasing the tensile strength of scaffolds. Upon increase of GTA concentration above 0.50% v/v GTA, the tensile strength of the scaffolds was significantly reduced. This was attributed to brittleness of the structures as a result of over-crosslinking and porous feature of the scaffolds. As expected, an increase of GTA concentration had a cytotoxic effect on cultured cells. However, it should be pointed out that the main objective of this study was optimising the *in-situ* gas foaming procedure and GTA was used as a model crosslinker with an effective, reliable, and rapid stabilising impact.

6. Acknowledgements

The authors acknowledge the support of Armourers & Brasiers' Gauntlet Trust (UK), The Fundação para a Ciência e Tecnologia (FCT) (project PTDC/EQU-EQU/114231/2009), PhD scholarship SFRH/BD/61450/2009, and contract IF/00442/2012.

7. References

1. Dagalakis, N.; Flink, J.; Stasikelis, P.; Burke, J. F.; Yannas, I. V. J. Biomed. Mater. Res. A 14, 511 (1980).

2. Dehghani, F.; Annabi, N. Curr. Opin. Biotechnol. 22, 661 (2011).

3. Kiran, E. J. Supercrit. Fluid 54, 296 (2010).

4. Barbetta, A.; Gumerio, A.; Pecci, R.; Bedini, R.; Dentini, M. - Biomacromolecules, 10, 3188 (2009).

5. Hesaraki, S.; Zamanian, A.; Moztarzadeh, F. J. Biomed. Mater. Res. B 86B, 208 (2008).

6. Gómez-Guillén, M. C.; Giménez, B.; López-Caballero, M. E.; Montero, M. P. Food Hydrocoll. 25, 1813 (2011).

7. Poursamar, A.; Hatami, J.; Lehner, A.; De silva, C.; Ferreira, F.; Antunes, A. P. M. Mater. Sci. Eng. C, 48, 63 (2015).

8. Kamel, R. A.; Ong, J. F.; Eriksson, E.; Junker, J. P. E.; Caterson, E. J. J. Am. Coll. Surg. 217, 533 (2013).

9. Supp, D. M.; Boyce, S. T. Clin. Dermatol. 23, 403 (2005).

10. Kim, B.S.; Park, I.K.; Hoshiba, T.; Jiang, K.L.; Choi, Y.J.; Akaike, T.; Cho, C.S.; Prog. Polym. Sci. 36, 238 (2011).

11. Choi, Y. S.; Hong, S. R.; Lee, Y. M.; Song, K. W.; Park, M. H.; Nam, Y. S. Biomaterials, 20, 409 (1999).

12. Mao, J.; Zhao, L.; de Yao, K.; Shang, Q.; Yang, G.; Cao, Y. J. Biomed. Mater. Res. A 64A, 301, (2003).

13. Boateng, J. S.; Matthews, K. H.; Stevens, H. N. E.; Eccleston, G. M. J. Pharm. Sci. 97, 2892 (2008).

14. Sun, S.; Lin, Y.; Weng, Y.; Chen, M. J. Food Compos. Anal. 19, 112 (2006).

15. Melling, M.; Pfeiler, W.; Karimian-Teherani, D.; Schnallinger, M.; Sobal, G.; Zangerle, C.; Menzel, E. J. Anat Rec 259, 327 (2000).

16. Temtem, M.; Silva, L. M. C.; Andrade, P. Z.; dos Santos, F.; da Silva, C. L.; Cabral, J. M. S.; Abecasis, M. M.; Aguiar-Ricardo, A. J. Supercrit. Fluid 48, 269 (2009).

17. De Carvalho, R. A.; Grosso, C. R. F. Food Hydrocoll. 18, 717 (2004).

18. Payne, K. J.; Veis, A. Biopolymers 27, 1749 (1988).

19. Jackson, M.; Choo, L.; Watson, P. H.; Halliday, W. C.; Mantsch, H. H. BBA-Mol. Basis Dis. 1270, 1 (1995).

20. Muyonga, J. H.; Cole, C. G. B.; Duodu, K. G. Food Chem. 86, 325 (2004).

21. Farris, S.; Song, J.; Huang, Q. J. Agr. Food Chem. 58, 998 (2010).

22. Chvapil, M. J. Biomed. Mater. Res. A 16, 245 (1982).

23. Carter, M. J. Applied Health Economics & Health Policy 12, 373 (2014).

24. Böttcher-Haberzeth, S.; Biedermann, T.; Reichmann, E. Burns 36, 450 (2010).

25. Barel, A.; Lambrecht, R.; Clarys, P. Curr. Probl. Dermatol. 26, 69 (1998).

26. Price, C. A. J. Dent. Res. 65, 987 (1986).

27. Wu, X.; Liu, Y.; Li, X.; Wen, P.; Zhang, Y.; Long, Y.; Wang, X.; Guo, Y.; Xing, F.; Gao, J. Acta. Biomater. 6, 1167 (2010).

28. Chiou, B.; Avena-Bustillos, R. J.; Bechtel, P. J.; Jafri, H.; Narayan, R.; Imam, S. H.; Glenn, G. M.; Orts, W. J. Eur. Polym. J. 44, 3748 (2008).

29. Nussinovitch, A. Biotechnol. Prog. 8, 424 (1992).

30. Khor, E. Biomaterials 18, 95 (1997).

31. Usha, R.; Ramasami, T. Thermochim. Acta. 356, 59, (2000).

32. Miles, C. A.; Ghelashvili, M. Biophys. J. 76, 3243, (1999).

33. Damink, L. H. H.; Dijkstra, P. J.; Luyn, J. A. V.; Wachem, P. B. V.; Nieuwenhuis, P.; Feijen, J. J .Mater. Sci.-Mater. M., 6, 460 (1995).

34. Enoch, S.; Leaper, D. J. Surgery (Oxford) 26, 31 (2008)

35. Yager,D.R.; Zhang,L.; Liang,H.; Diegelmann,R.F.; Cohen,K., J. Invest. Dermatol. ;107; 743 (1996).